

PACS: 78.20.-e

Dielectric, ferroelectric and piezoelectric properties of sputtered PZT thin films on Si substrates: influence of film thickness and orientation

T. Haccart, E. Cattan, D. Remiens

IEMN - DOAE - MIMM. UMR CNRS 8520 Université de Valenciennes ZI petite savate, 59600 Maubeuge, France
e-mail: denis.remiens@univ-valenciennes.fr

Abstract. Lead titanate zirconate $\text{Pb}(\text{Zr},\text{Ti})\text{O}_3$ (PZT) thin films were deposited on platinized silicon substrates by r.f. magnetron sputtering and crystallized with preferred (110) or (111) orientation by conventional annealing treatment. The film structure evolution was observed as a function of the film thickness. Whatever the film thickness in the range $0.07 - 3 \mu\text{m}$, the preferred orientation of the film is maintained. The film microstructure and, in particular, grain sizes varied with the film thickness; more precisely, grain sizes increases, both for (111) and (110) films with the film thickness. The electrical properties such as dielectric, ferroelectric and piezoelectric ones were systematically evaluated functions of the film thickness and their orientation.

The relative dielectric constant increases with the film thickness; a saturation value of 920 is attained for film thicknesses higher than $0.6 \mu\text{m}$ independently of the film orientation.

The ferroelectric properties seems to be independent of the film orientation; the coercive field decrease with increasing the film thickness to attain a minimum value of 30 kV/cm for films thicker than $1 \mu\text{m}$. The remanent polarization increases with the film thickness and reaches the maximum value of $20 \mu\text{C/cm}^2$.

An increase in the piezoelectric constant e_{31} with increasing the film thickness was observed for two types of films. For films thicker than $0.6 \mu\text{m}$, the e_{31} coefficient remains constant: $e_{31\text{eff,rem}} = -4.5 \text{ C/m}^2$ (which corresponds to $d_{31\text{eff,rem}} = -38 \text{ pm/V}$). Identical behavior is observed for the $d_{33\text{eff}}$ coefficient but no saturation effect with the film thickness is observed. The ferroelectric domain walls motion and the interfacial effects could explain partly the observed behavior.

Keywords: ceramic thin film; sputtering; film thickness and orientation; dielectric, ferroelectric and piezoelectric properties.

Paper received 14.01.02; revised manuscript received 20.02.02; accepted for publication 05.03.02.

1. Introduction

Lead oxide-based ferroelectric films have attracted considerable attention for potential microelectronic and electromechanical applications; in particular, PZT materials are the most popular candidates. PZT thin films with different composition (ratio Zr/Ti), depending on

the desired applications have been extensively studied. The main device applications were semiconductor non-volatile memories [1], pyroelectric detectors [2] and piezoelectric sensors [3] and actuators [4]. For these later applications, the PZT films composition is generally chosen on the morphotropic phase boundary, i.e. a Zr/Ti ratio the order of 50/50.

For device applications, it is imperative to perfectly

know the influence of the film characteristics such as:

- the structure (epitaxial or polycrystalline films with preferred orientation)
- the microstructure (grain size) and the interfaces,
- the thickness, ...

on the electrical properties. For example, for Micro Electro Mechanical Systems (MEMS) applications, the film thickness must be in the order of 1 μm or more [5]; on the contrary, for nonvolatile memories, the film must be very thin⁶ (0.2 – 0.3 μm). It is evident that the thickness must have a strong influence on the film electrical properties.

The structure and the microstructure of PZT films were controlled by many parameters: the growth technique, the substrate nature and orientation, the presence of a seed layer or an electrode surface. The electrode surface has the function to decrease the nucleation energy for a given crystallographic orientation of the nucleus. It has been clearly established that the formation of the perovskite phase was nucleation controlled. The film orientation and thickness have also an influence on the physical properties, and it is necessary to precisely evaluate this dependence in order to improve the device performance.

Many authors have described the influence of PZT films orientation on their electrical properties but the results were in many cases in contradiction. For example, we can find in the literature that (111)-oriented PZT films are higher coercive field than (100) films, but the opposite situation has been also published [7,8]. Identical situation for the film thickness effect^{9,10} was ascertained. Concerning the evaluation of the piezoelectric coefficients e_{31} , d_{31} and d_{33} dependence with the PZT film thickness there is a limited number of papers [11,12].

So, in this article we have systematically studied PZT films deposited by r.f. magnetron sputtering followed by a post-annealing treatment on Pt metallized silicon substrates:

- the influence of the film thickness on their structural and micro structural properties,
- the influence of the film thickness and orientation on their electrical properties: dielectric, ferroelectric and piezoelectric.

Some tentative behavior explanations are made, and a correlation between the electrical properties and the microstructure by the way of the existence of an interfacial layer between the film and the substrate as well as the domain walls motion is given.

2. Film deposition and characterization

The r.f. magnetron sputtering system, described previously [13], was used to prepare PZT thin films; the films composition, i.e. the (Zr/Ti) ratio, was fixed to 54/46 (near the morphotropic phase boundary). It is well known that in the bulk ceramics the best piezoelectric performance is obtained for this composition.

The sputtering target was a mixture of PbO, TiO₂ and

ZrO₂ in the stoichiometric composition (without lead excess); the targets were obtained by uniaxially cold pressing.

The PZT films were deposited onto oxidized silicon (SiO₂ - 3000 Å)- (100) n-type Si substrates coated with Ti/Pt electrodes. The thickness of the Ti and Pt layers was 100 and 1500 Å, respectively. More precisely, we have deposited an oxydized titanium, i.e. TiO_x, layer as an adhesion film for the Pt layer on SiO₂. The main objective is to limit the diffusion of titanium through Pt; it is well known that the diffusion velocity of TiO_x is lower than Ti; then this procedure can stabilize the substrate during the PZT crystallization post-annealing treatment. With the same idea (stabilization of the substrate), just before the PZT deposition, we have made an annealing treatment of the Si/SiO₂/TiO_x/Pt substrates at a temperature higher to the post-annealing PZT treatment. A more complete description of the substrate preparation is given elsewhere [14]. Hence, with this precaution, we can suppose that the substrates used in this experiment are similar and stable. But, as we can see later, this is not the case and the PZT films orientation can varied between two depositions run. We think that only the substrate and, in particular, the bilayers TiO_x/Pt can be responsible for this modification. More complete studies are necessary to understand the substrate evolution, which appears during the annealing treatment of the PZT films.

Table. Typical sputtering parameters for the PZT films growth and post-annealing conditions.

Target composition	Zr/Ti = 54/46 – without lead excess
Target diameter (mm)	76
r.f. power density (W /cm ²)	3
Gas pressure (mT)	30 (Ar)
Interelectrodes distance (mm)	60
Substrate temperature (°C)	25-140 (ion bombardment)
Annealing temperature (°C)	625
Annealing time (min.)	30
Atmosphere	Air

The PZT sputtering conditions are summarized in Table 1; they are optimized in order to obtain a stoichiometric film (measured by Energy Dispersion Spectroscopy) and a relatively important growth rate (for an oxide material). It was estimated to 30 E/min; for higher r.f. power density (which influence strongly the growth rate) some cracks appear on the target, in particular, in the erosion area (magnetron system). The films were grown without substrate heating and so they are amorphous; a post-annealing treatment is necessary to crystallize the PZT in the desired phase, i.e. in the perovskite phase.

We have been optimized two processes [15]:

- the conventional annealing in a tubular furnace,
- the rapid thermal annealing .

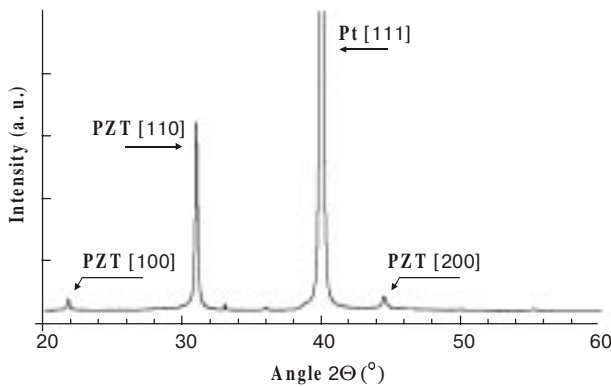


Fig. 1a. Typical XRD patterns example of a 0.7 μm thick (110)-oriented PZT.

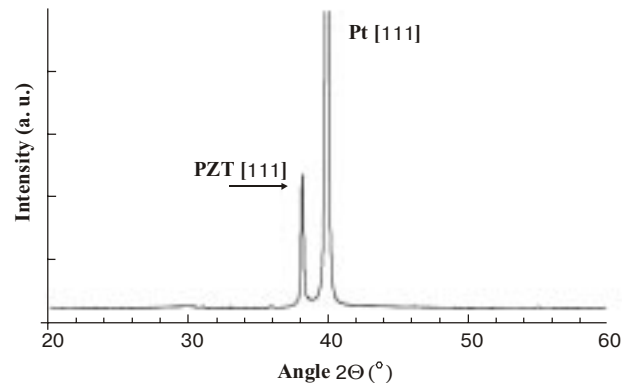


Fig. 1b. Typical XRD patterns example of a 0.7 μm thick (111)-oriented PZT.

In this paper, we present only the results relative to the conventional treatment. The typical annealing conditions, whatever the film thickness, were given in table; no cracks appear and the films composition are stoichiometric (in particular the lead content) after this treatment.

The film structure was analyzed by X-Rays Diffraction (XRD) in the q - $2q$ configuration with the $\text{CuK}\alpha$ radiation. Fig. 1a shows the XRD pattern of a PZT film, the film thickness is of the order of 0.7 μm . The film is perfectly crystallized in the perovskite phase, and no pyrochlore phase was detected. The film is polycrystalline, i.e. randomly oriented, but the (110) intensity peak is largely superior to the others (like PZT ceramics), and we consider that this sample has a preferred (110) orientation. Fig. 1b shows also an XRD pattern of a PZT film (0.7 μm thick) which has suffered the same elaboration process as the precedent film. As previously, the film is completely crystallized in the perovskite phase, but it is now (111) preferentially oriented. At present, it is difficult to explain why the crystallographic orientation is different between the PZT films. The sputtering conditions are identical and the difference could be attributed to the substrate. An hypothesis will be that the degree of oxidation (x) of the TiO_x layer varied between the wafers; so, since the TiO_x diffusion rate is very sensitive to x , we can suppose that the diffusion of TiO_x differs between the wafers and the difference of the «penetration depth» of TiO_x through Pt (the extreme case is the encapsulation of Pt, i.e. presence of TiO_x on the substrate surface) could influence the PZT crystallization [16,17]. With the same idea, the thickness of the TiO_x and Pt layers can be also varied in the deposition processes; in particular, the TiO_x layer thickness is very fine (100 \AA) and a little increase (decrease) of the thickness could favors the TiO_x diffusion through the Pt joints grain and so modify the PZT crystallization [17,18]. These hypotheses must be confirmed more precisely, but certitude is that we can reproduce PZT films with (111) or (110)-preferred orientation. Another possibility would be the differences in whether the nucleation occurred from the bottom electrode (where (111) orientation would be favored) or from some other places (perhaps the surface), which would favor randomly oriented PZT, i.e. (110) PZT films [18].

We have studied the evolution of the (110) and (111) PZT films orientation as a function of the film thickness, which varied in the range 0.07– 3.2 μm . A typical example is given in Figs 2a and 2b, which shows respectively the X ray diffraction structure evolution of (110) and (111)-PZT film. For the (111)-oriented films, the degree of orientation $a(111)$ (defined as a $(111) = I(111) / \sum I(hkl)$) varied between 98 and 96 % for respectively a film thickness of 0.09 and 2 μm . Identical results were obtained for the (110) PZT films. To complete this study, we have followed the structural film evolution with the thickness by varying the X-ray incident angle (α_i). The incident angle controls the analyzed film thickness; more precisely, when the incident angle decreased, the analyzed film depth decreased. An example is given by Fig. 3 for a (110) film; the wavelength of the X-rays used in this experiment is 1.789 \AA (cobalt cathode), which explains the variations of the perovskite plane diffraction angles in comparison to the X-ray pattern shown in Fig. 1 (Cu cathode).

For comprising α_i between $[0.3^\circ\text{-}2^\circ]$, the film is always (110)-oriented and confirms that the film orientation is maintained constant across the thickness. Identical results were obtained for the (111)- oriented films. We can also remark that, in contradiction to J.C. Kim works [19], the pyrochlore phase doesn't appear at the film surface, i.e. for very low α_i value ($\alpha_i = 0.3^\circ$).

We have also evaluated the evolution of the film microstructure as a function of the film thickness. Firstly, we have compared the microstructure of a (111) and (110)-oriented PZT film. The morphology of these two types of films is very different; the grain size of the (110)-oriented films is large and the grain joints surface is large, too. In comparison, the grain size of the (111)-oriented film is very fine, and their distribution is more homogeneous. It is very difficult to compare our results with those published in literature, since the films thickness are different and the films is often obtained by sol-gel. Some results are in contradiction; for example, Brooks et al. [20] and Liam et al. [9] have observed that the film microstructure is very fine and homogeneous for (111)-oriented PZT films in comparison to (100) films. Aoki et al. [10] has observed exactly opposite results. Kurchania et al. [11] have observed identical results as those presented here, i.e. the

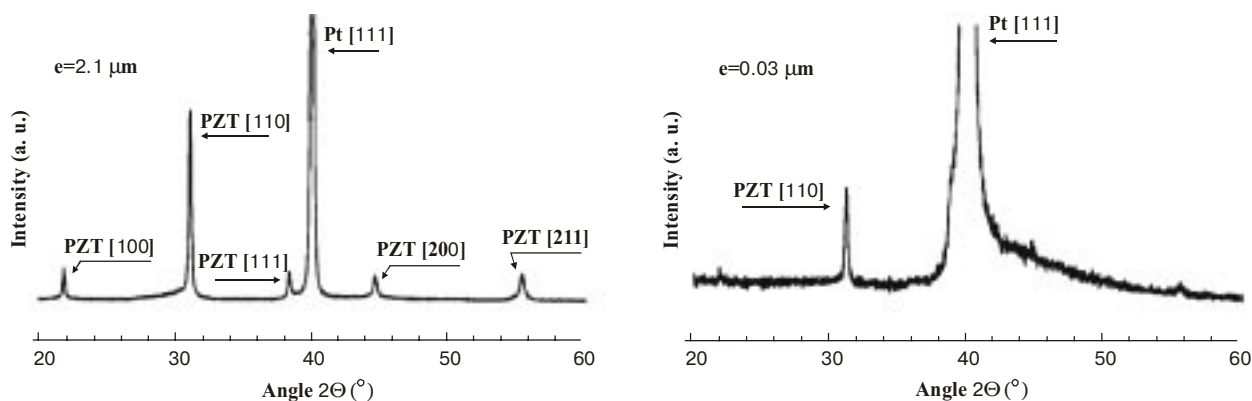


Fig. 2a. Evolution of the XRD patterns of a (110)-oriented PZT film function of the thickness.

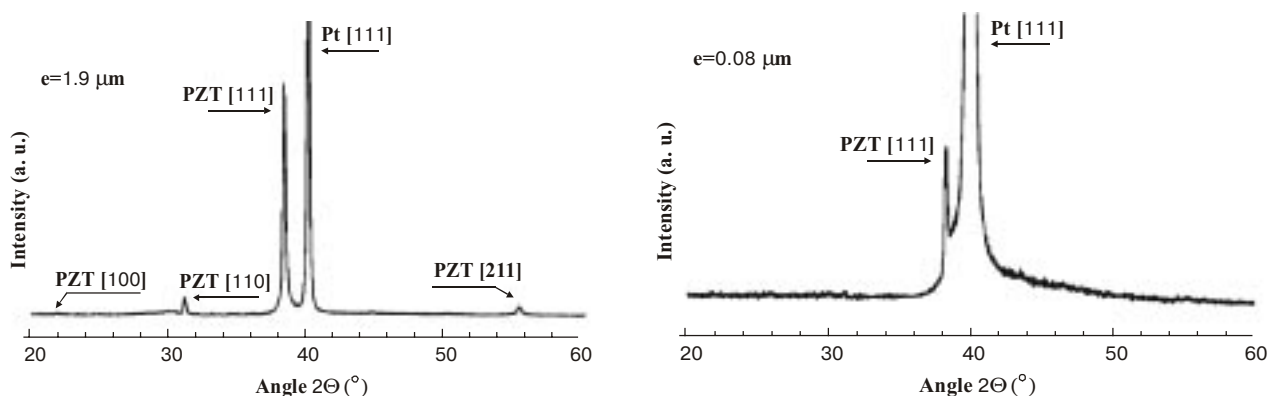


Fig. 2b. Evolution of the XRD patterns of a (111)-oriented PZT film function of the thickness.

same difference between (111) and (110) PZT films microstructure, but grain sizes are smaller in their works.

Some authors have studied the evolution of grain sizes as a function of the film thickness. The obtained results are also in contradiction in some cases. Lian et al. [9] and Taylor et al. [21] have observed some modification of the film microstructure; the films are deposited by sol-gel and the thickness varied between 0.37 to 1.8 μm . For PZT films obtained also by sol-gel, Kim et al. [19] and Kurchania et al. [11] have observed a grain growth with the film thickness in the range 0.3 to 2 μm ; their results are in perfect agreement with the observations of Chen et al. [22] and Fujisawa et al. [23]. Some explanations are given concerning the variation of grain sizes with the film thickness; the decrease of the residual stresses when the thickness increased could be a response.

Our results show an important grain size evolution with the film thickness; an illustration is given by Fig. 4. Fig. 4a is relative to (110)-oriented PZT films; the film thickness varied between 0.3 to 2 μm . The grain size increased with the film thickness and their distribution is not homogeneous. Identical distribution has been observed for PZT films elaborated by sol-gel [22]. The grain growth with the film thickness for (111)-oriented PZT films is shown in Fig. 4b; as we have mentioned previously, the grain size is smaller in comparison to PZT (110). For example, a 0.3 μm thick PZT films have an

average grain sizes of 0.1 and 0.2 μm for respectively a (111) and (110) orientation. It attains 0.6 and 1 μm for respectively a (111) and (110)-oriented films of 2 μm thick. To explain this increase of the grain size with the film thickness some authors have taken into account the existence of the stresses in the films and the possible grain disorientation with the film thickness increase [9, 24, 25]. Since in our case, the crystalline orientation is maintained constant with the thickness (in the thickness range studied), we can suppose that the observed evolution is mainly related the decrease of stresses when the film thickness increases.

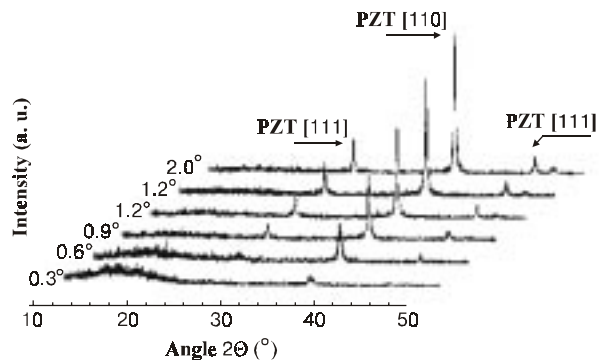


Fig. 3. (110)-oriented PZT film structural evolution with thickness by varying the X-ray incident angle (Cobalt cathode).

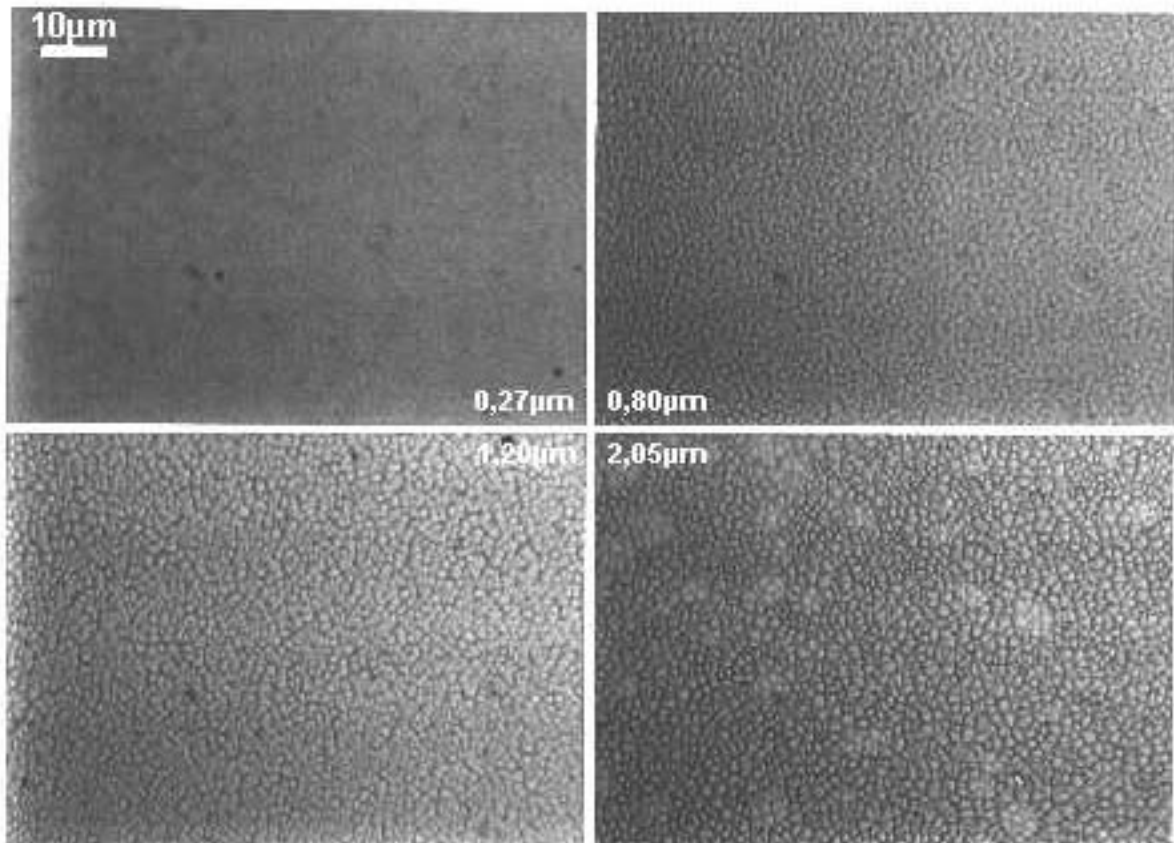


Fig. 4a. Evolution of grain sizes with the film thickness for a (110)-oriented PZT films.

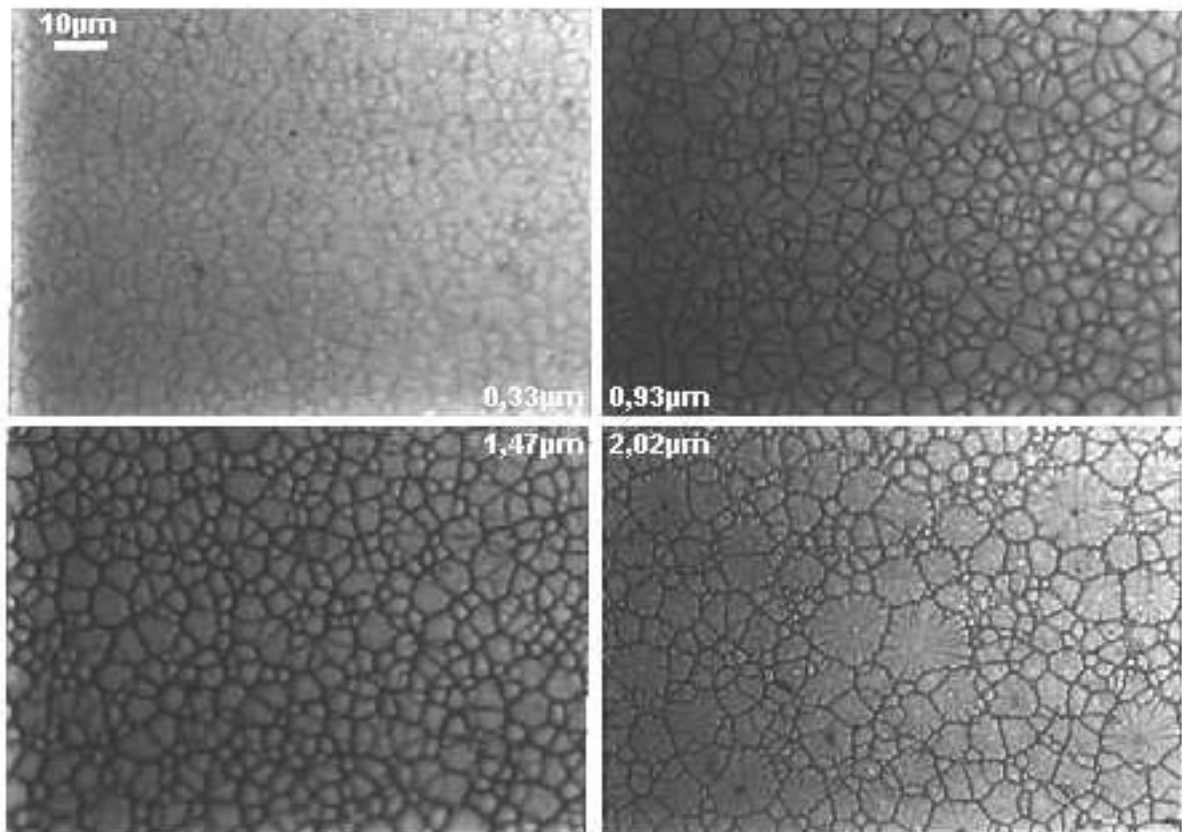


Fig. 4b. Evolution of grain sizes with the film thickness for a (111)-oriented PZT films.

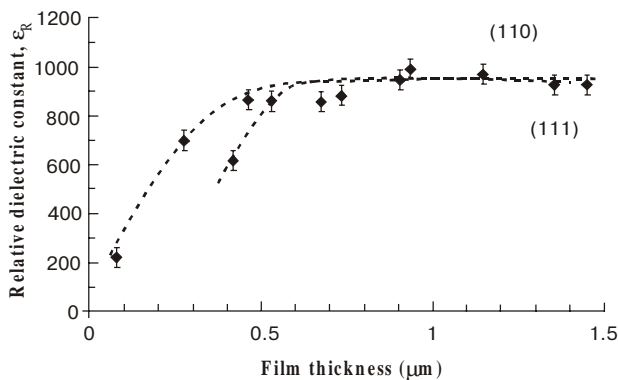


Fig. 5. Evolution of the relative dielectric constant function of the film thickness for a (110) and a (111)-oriented PZT films.

The microstructure variation with the film thickness must have some issues on the electrical properties of the films. We have evaluated this contribution and also the influence of the film orientation and thickness.

3. Electrical characterization

The PZT films were systematically characterized as a function of the film orientation and thickness in terms of dielectric constant, ferroelectric and piezoelectric properties. The embedded beam method and a double beam Michelson interferometric system are used to measure the e_{31} and d_{33} piezoelectric coefficients, respectively [26, 27]. For electrical properties evaluation, platinum top electrodes of 0.2 μm thickness were formed by photolithography and sputtering (lift-off process). The electrode surface is large for the piezoelectric measurements; it is of 1 mm²; for the dielectric and the ferroelectric evaluations we used 150 μm diameter circular electrodes.

A- Dielectric constant

The relative dielectric constant, ϵ_r , were measured at 1 kHz with an LCR meter at room temperature. In order to not modify the polarization state of the film, we have applied a very weak ac voltage (100 mV). The results are presented in Fig. 5 both for (110) and (111)-oriented films.

The ϵ_r evolution with the film thickness is similar for two types of films; the curve can be decomposed into two parts: for the film thickness thinner than 0.6 μm, ϵ_r increases linearly. For thicker films (> 0.6 μm), ϵ_r attains a saturation value of 920 independently of the film orientation. Many papers have been published on this subject and our results are conformed to the observed tendency [28,29,30]: An increase of ϵ_r with thickness takes place until it attains a saturation value for a threshold thickness (ϵ_{th}). The ϵ_{th} values are different in literature; typically ϵ_{th} is of the order of 0.3–0.5 μm; in our case ϵ_{th} is equal to 0.5–0.6 μm whatever the film orientation. The origin of ϵ_r variation with the film thickness can be attributed to different factors:

- The existence of a material with a very low dielectric constant (non-ferroelectric state also called “dead” layer) at

the interface between the film and the Pt bottom electrode can explain the low ϵ_r -values of the structure for very thin PZT films¹⁸. For example, we have measured $\epsilon_r = 225$ for a film thickness of 0.08 μm. When the film thickness increases this effect becomes minor.

- The correlation between the grain size and the relative dielectric constant, i.e. an increase of the grain size, resulting from an increase of the thickness, induces an increase of ϵ_r [23,31].

The increase of ϵ_r with the film thickness is directly related to the decrease of the stresses with the film thickness increase [28].

Cho et al. [29] and Xu et al.[32] have made a complete study of the PZT film relative dielectric constant and loss factor ($\tan \delta$) evolutions with the thickness as functions of the applied electric field amplitude (E_{ac}) as well as the temperature. In their analysis, they introduce the intrinsic and extrinsic contributions into the PZT film dielectric properties. More precisely, the lattice contribution corresponds to the intrinsic part and domain wall motion corresponds to the extrinsic properties. The dielectric measurements at a very low temperatures (close to 0K) «block» the domain walls and only the intrinsic contribution must be taking into account in the dielectric response. An excellent paper published recently by S. Hiboux et al. described also different contribution deduced by the C(V) measurements [33]. The dielectric evolution with the applied electric field is related to the domain wall motion. Their result shows that the extent of domain wall motion increased with film thickness. The intrinsic effects contribute to all films and show a saturation whatever the film thickness, so the difference in the observed dielectric permittivity values is attributed to the extrinsic contribution. This behavior could be explained by the existence of an interfacial layer between the film and the substrate.

The composition and the thickness of this interfacial zone are unknown, and it doesn't present ferroelectricity. The film can be decomposed into two parts: the interfacial layer and the ferroelectric layer. The main consequence is that the number of domains, which contribute to the extrinsic effect, is limited for films thickness thinner than 0.6 μm, i.e. the “effective” PZT ferroelectric film thickness is much less than 0.6 μm. The presence of this interfacial layer has also a negative effect on the domain wall mobility by the introduction of pinning centers, the domains preferentially localized near this interfacial layer are blocked. When the film thickness increases, the domain density increases, and then the extrinsic effect increases. The thickness of the “effective” ferroelectric film becomes larger than the “dead” zone. The pinning centers localized near the interface have also a minor effect when the thickness increases. The microstructure evolution with the film thickness, and, in particular, the increase of the grain size induce an enhancement of the domain wall motion since the joints grain density, which act as pinning center, decreases. The ϵ_r evolutions, in the first part of the curve (Fig. 5), can be explained by these different contributions; in particular, the interfacial layer plays a major role. The fact that ϵ_r attains a saturation value (for films thicker than ϵ_{th}) can't be explained com-

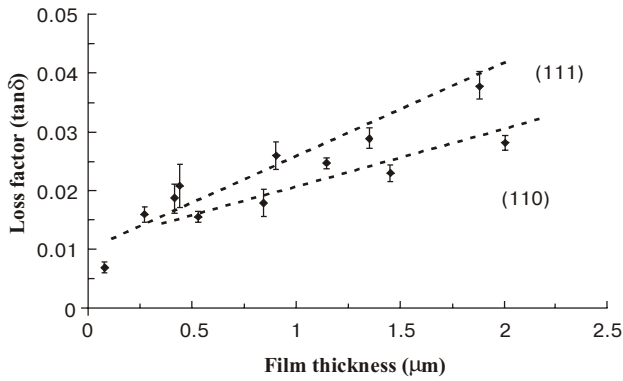


Fig. 6. Evolution of the loss factor function of the film thickness for a (110) and a (111)-oriented PZT films.

pletely by these arguments and complementary studies are necessary [32].

The evolutions of the loss factor, $\tan \delta$, with the film thickness are presented in Fig. 6. There are many contributions to the dielectric losses. The loss factor corresponds to the losses induced by the energy dissipation during the domain wall motions [29, 32], and there are also contributions from conductivity. The loss factor of the (111)-oriented PZT films is very similar to the (110) PZT films for films thinner than $0.6 \mu\text{m}$; it is of the order of 1.8%. For thicker films, $\tan \delta$ increases linearly for the two types of films, but it seems higher for the (111) orientation. It is well known that in bulk hard and soft PZTs, as the domain mobility increases, the dielectric losses increase. Then, these results are in perfect agreement with the increases of the permittivity with the film thickness but we have no explanation concerning the difference observed between the (111) or (110) oriented films; may be it is connected with the interfacial layer nature, thickness. No $\tan \delta$ saturation is detected as on the ϵ_r variation with the film thickness.

B- Ferroelectric properties

The ferroelectric nature of the films was examined by observing the hysteresis loop taken at room temperature by means of a RT 6000 system (Radian Technology). Polarization reversal is generally taken as a measure of the degree of ferroelectricity.

Fig. 7 shows the evolution of the average remanent polarization ($P_{r,aver.} = P_r^+ - P_r^- / 2$) as a function of the film thickness for the two types of films. The remanent polarization increases with the film thickness and attains a saturation value for films thicker than $0.6 \mu\text{m}$, whatever the film orientation; typically, the remanent polarization is of the order of $20 \mu\text{C}/\text{cm}^2$. The maximum polarization (P_M) variations are similar to those of $P_{r,aver.}$ and P_M is equal to $40 \mu\text{C}/\text{cm}^2$, independently of the film orientation, for films thicker than $0.6 \mu\text{m}$. The variations of the coercive field with the film thickness are presented in Fig. 8. The coercive field decreases with the film thickness and a saturation value of $30 \text{ kV}/\text{cm}$ is measured for films thicker than $0.7 \mu\text{m}$. The variations are similar for two types of films except for the very thin film ($< 0.7 \mu\text{m}$) where the (111)-oriented PZT film

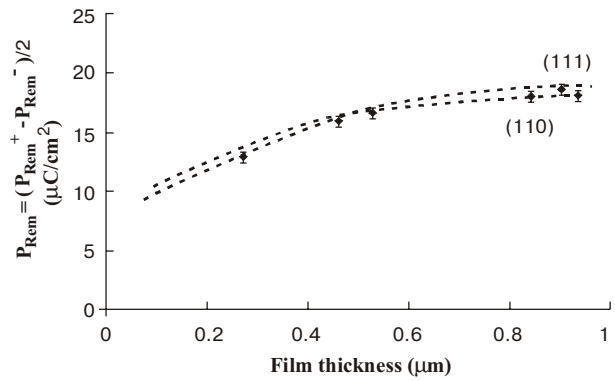


Fig. 7. Evolution of the average remanent polarization ($P_{av.rem.}$) function of the film thickness for a (110) and a (111)-oriented PZT films.

presents higher coercive field. These results are in perfect agreement with those published in the literature [30,32,34]. For very thin film, the presence of an interfacial layer (“dead” layer) between the PZT film and the substrate degrades the ferroelectric performances; when the PZT film thickness increases, these layer have a less effect. So, the domain wall mobility increases, which induces an improvement of the domain switching; as a consequence, the coercive field decreases.

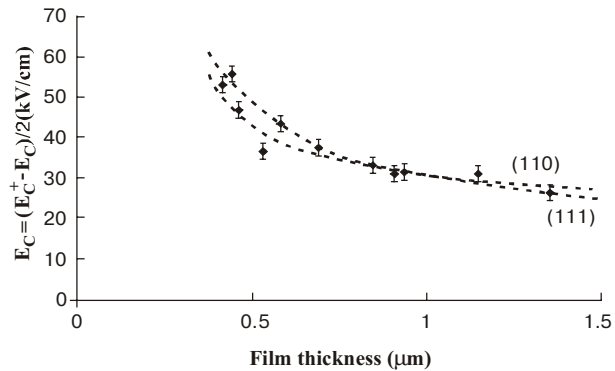


Fig. 8. Evolution of the coercive field (E_C) function of the film thickness for the two type of films.

Fig. 9 shows the evolution of the internal electric field ($E_{int.}$) as a function of the film thickness. The behavior is similar for Both types of films: a decrease with the film thickness, but in general, the internal electric field is more important for a (110) PZT film rather than for a (111) film. A saturation is observed for films thicker than $1 \mu\text{m}$. The existence of this internal electric field is often attributed to the space charges, the oxygen defects and the stresses [35]. It is admitted that the space charges and the oxygen vacancies are located near the bottom electrode and act as pinning centers. Therefore, the maximum of the internal and the coercive fields are obtained for very thin films; the space charges influence is neglected when the film thickness increase, i.e. for film thickness higher than $1 \mu\text{m}$ in our case and the hysteresis loops asymmetry disappears.

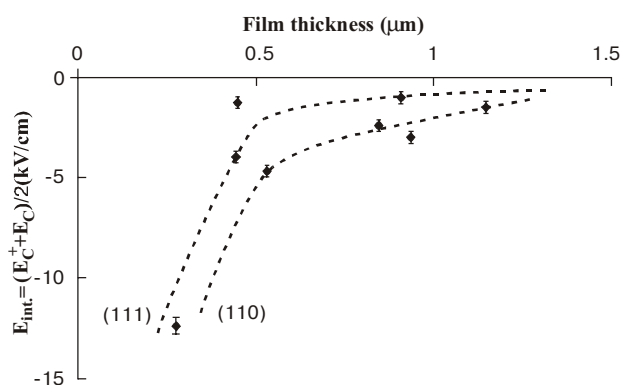


Fig. 9. Evolution of the internal electric field (E_{int}) function of the film thickness for the two types of films.

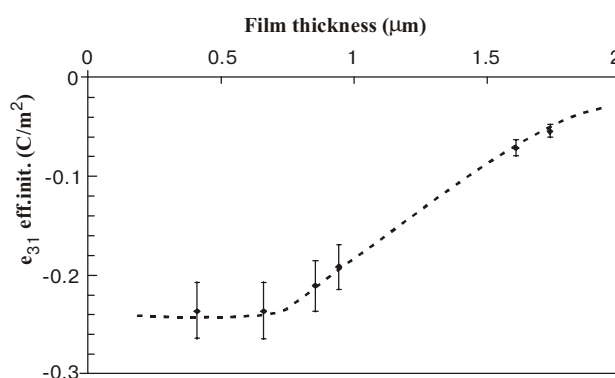


Fig. 10. Evolution of the initial effective e_{31} coefficient ($e_{31\text{eff.init.}}$) function of the films thickness.

C- Piezoelectric properties

We have systematically evaluated the e_{31} and the d_{33} piezoelectric coefficients. As the films are clamped by the substrate, the measured coefficients are effective ($e_{31\text{eff.}}$ and $d_{33\text{eff.}}$), and it is difficult to compare the coefficients values with those obtained on bulk ceramics [36]. The measurements are made for both types of film orientation and the obtained values are very similar. So, we present only the results relative to (110)-oriented PZT films.

The details for the experimental set-up as well as for the beam embedded method [37] ($e_{31\text{eff.}}$ measurement) and for the double beam interferometric method [38] ($d_{33\text{eff.}}$ measurement) are described previously. From the $e_{31\text{eff.}}$ measured values, we can deduce, by a simple calculation, which used the electromechanical properties of the PZT bulk ceramics and the Si substrate, the $d_{31\text{eff.}}$ piezoelectric coefficient.

Fig. 10 shows the initial $e_{31\text{eff.}}$ (noted $e_{31\text{eff.init.}}$) evolution with the film thickness. The $e_{31\text{eff.init.}}$ corresponds to the piezoelectric response of the film without poling treatment (virgin film). For films thinner than $0.6\ \mu\text{m}$, the $e_{31\text{eff.init.}}$ is constant; it is in the order of $-0.25\ \text{C/m}^2$ ($d_{31\text{eff.}} = -2.2\ \text{pm/V}$). For films thicker than $0.6\ \mu\text{m}$, the $e_{31\text{eff.init.}}$ decreases continuously; for example, $e_{31\text{eff.init.}}$ is equal to $-0.05\ \text{C/m}^2$ ($d_{31\text{eff.}} = -0.45\ \text{pm/V}$) for a $1.75\ \mu\text{m}$ thick PZT film. The existence of this piezoelectric signal from PZT films has been observed by some authors [39,40,41]; it is directly related to the preferential orientation of some domains in the film induced by the internal electrical field. An important result is that the $e_{31\text{eff.init.}}$ is maximum for films thinner than $0.6\ \mu\text{m}$ which corresponds to film thickness where the internal electric field is maximum (Fig. 9). The deposition of PZT films by sputtering leads to an orientation of the ferroelectric domains, which induced this piezoelectricity in the unpoled films. This phenomenon, also observed for PZT films deposited by other techniques, is currently called «self-polarization»

effect. The existence of this “self polarization” is related to non-uniformly distributed oxygen vacancies [42], the formation of dipoles with oxygen vacancies and negatively charged acceptors [43], and also to non-uniform compensation of oxygen vacancies. This characteristic of ferroelectric thin films is not observed in bulk ceramics that have zero net polarization due to the initial random orientation of ferroelectric domains inside the grains. The preferential orientation of domains in virgin films is incomplete since a polishing treatment induces an optimization of their piezoelectric performances. The polishing treatment has been optimized in terms of applied electric fields and polishing time: the polishing electric field is near the saturation electric field and the polishing time is fixed to 20 min at room temperature [44]. The $e_{31\text{eff.}}$ evolution as a function of the film thickness is given in Fig. 11; the $e_{31\text{eff.}}$ coefficient presented in this curve corresponds to the remanent coefficient ($e_{31\text{eff.rem.}}$) since the DC poling voltage is removed when we want to acquire the piezoelectric signal. The variations can be decomposed into two parts: an increase of $e_{31\text{eff.rem.}}$ for films thinner than $0.6\ \mu\text{m}$; in the second part of the curve, the piezoelectric coefficient remains constant in the order of $-4.5\ \text{C/cm}^2$ (the $d_{31\text{eff.rem.}}$ associated is $-38\ \text{pm/V}$). The increase of $e_{31\text{eff.rem.}}$ is directly related to the domain contribution, which increases with the film thickness. The maximum is attained for a PZT film thickness of $0.6\ \mu\text{m}$ as for the dielectric permittivity. An illustration of the $e_{31\text{eff.}}$ evolution with the film thickness is given in Fig. 12, which shows the $e_{31\text{eff.}}$ piezoelectric hysteresis loops for two PZT films of different thickness. The experimental procedure is described elsewhere; an important asymmetry is observed as in the ferroelectric hysteresis loops [35]. The $e_{31\text{eff.rem.}}$ saturation value detected for films thicker than $0.6\ \mu\text{m}$ was not observed in the $d_{33\text{eff.}}$ variation. An example is given in Fig. 13; typically, $d_{33\text{eff.rem.}}$ is of the order of $45\ \text{pm/V}$ and

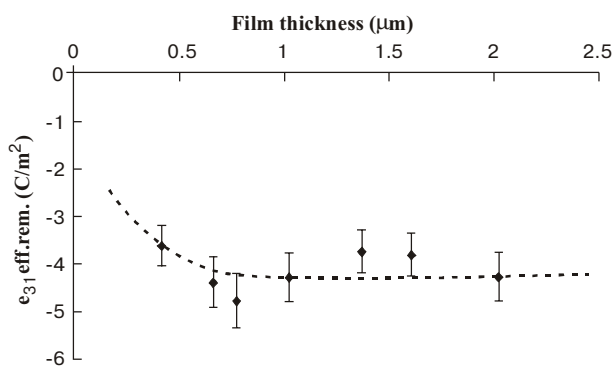


Fig. 11. Evolution of the remanent effective e_{31} coefficient ($e_{31,eff.rem.}$) function of the film thickness.

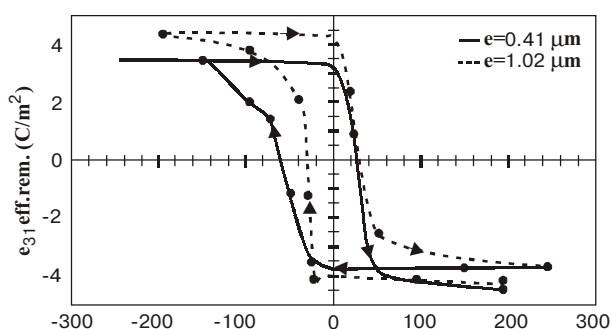


Fig. 12. Typical example of piezoelectric e_{31} hysteresis loops for PZT films of different thickness.

80 pm/V for PZT films of 1 and 1.7 μm thickness respectively. A limited number of papers have been published concerning the dependence of the e_{31} and d_{33} piezoelectric coefficients with the film thickness and no explanation has been given. Lee et al.[45] have shown that the d_{31} coefficient increases with the film thickness but saturates for PZT films thicker than 1 μm . Liam et al.[9] and Taylor et al.[21] have presented some d_{33} measurements on PZT films with different thickness, d_{33} increases monotonically with the film thickness increase.

Conclusion

A study on the film orientation and thickness effects on the PZT structure, microstructure and electrical properties is given in this paper. The PZT films are fabricated by r.f. magnetron sputtering followed by a conventional annealing treatment on Si/SiO₂/TiO_x/Pt substrates. The fabrication processes are similar for all the films presented in this paper: bottom electrode deposition, pre-sputtering, sputtering, and annealing conditions. But even with this rigorous procedure two preferred PZT films orientation: (110) and (111) are obtained. This structural difference is probably due to an evolution of the TiO_x/Pt bilayers (diffusion of the TiO_x through the Pt joints grain) during the PZT crystallization treatment.

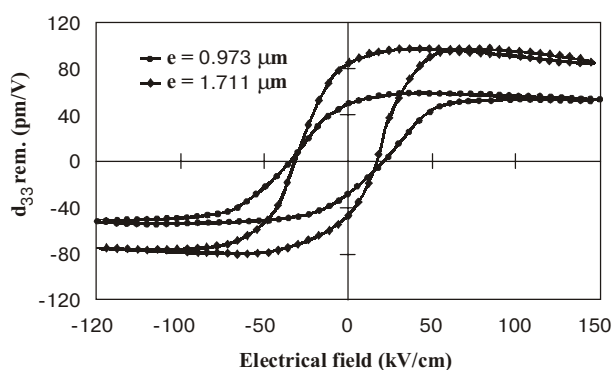


Fig. 13. Typical example of piezoelectric d_{33} hysteresis loops for PZT films of different thickness.

Transmission Electron Microscopy is now in progress to identify the interfacial layer and may be enable understand the observed structural modification.

No change in the structural evolution was observed with the film thickness (in the thickness range studied): the preferred orientation (111) or (110) is maintained whatever the film thickness. In terms of micro-structure, the grain size was larger for (110) PZT films in comparison to (111) oriented films; an increase with the film thickness is systematically observed.

Variations of the main electrical properties variation can be summarized as follows:

- The relative dielectric constant increase with the film thickness whatever the film orientation and a saturation value (920) is attained for film thickness higher than 0.6 μm . The loss factor increases also with film thickness, but no saturation effect is observed.
- The ferroelectric properties seem to be independent of the film orientation, and a marked dependence with the film thickness is observed. In particular, the coercive field decrease when the film thickness attains the saturation value of 30kV/cm for film thickness higher than 1 μm . The internal electric field decrease with the film thickness. The remanent and the maximum polarization increase with the film thickness.
- The virgin films (without polishing treatment) present piezoelectric activity. This piezoelectric response is maximum for film thinner than 0.6 μm , where the internal electric field is also maximum. The e_{31} and d_{33} piezoelectric coefficients increase with the film thickness and a saturation effect is observed only for the e_{31} coefficient.

The electrical properties dependence with the PZT film thickness can be explained by the existence of an interfacial layer also called a "dead" layer (which reduce the "effective" thickness of the ferroelectric material), the contribution of the domain structure (increase of the domain density and the domain wall mobility), the pinning centers and the microstructure (grain size, joint grain.). A better understanding of the PZT film properties evolution with the film thickness necessitates to study the dynamic behavior of the domains. To this fact, studies are now in progress in our laboratory concerning the evolution of the domain motion by using atomic force microscopy in the contact and no contact mode.

References

1. J.F. Scott, "Status report on ferroelectric memory materials", // *Integrated Ferroelectrics*, 20, 15-23 (1998).
2. S.L.Bravina, N.V. Morozovsky, "Pyroelectricity in some ferroelectric semi conductors and its applications", // *Ferroelectrics*, 118, 217-224, (1991).
3. P.Muralt, "Ferroelectric thin films for microsensors and actuators ; a review", // *J.Microeng.*, 10, 136-146, (2000).
4. D. Eichner, M.Giousouf, W. Von Munch, "Measurements on micromachined silicon accelerometers with piezoelectric sensor action", // *Sensors & Actuators*, 76, 247-252, (1999).
5. A. Schroth, C. Lee, S.Matsumoto, R. Maeda, "Application of sol-gel deposited thin PZT film for actuation of 1D and 3D scanners", // *Sensors & Actuators*, 73, 144-152, (1999).
6. S-K. Hong, C.S. Hwang, O.S. Kwon, N.S. Kang, "Polarity dependent rejuvenation of ferroelectric properties of integrated SrBi₂Ta₂O₉ capacitors by electrical stressing", // *Appl.Phys.Lett.*, 76(3), 324-326, (2000).
7. J.F.M. Cillessen, M.W. Prins, R.M. Wolf, "Thickness dependence of the switching voltage in all-oxide ferroelectric thin film capacitors prepared by pulsed laser deposition", // *J.Appl.Phys.*, 81(6), 2777-2783, (1997).
8. S- Yan Chen, I-Wei Chen, "Comparative role of metal-organic decomposition-derived [100] and [111] in electrical properties of Pb(Zr,Ti)O₃", // *Jpn.J.Appl.Phys.*, 36(7A), 4451-4458, (1997).
9. L. Lian, N.R. Sottos, "Effect of thickness on the piezoelectric and dielectric properties of lead zirconate titanate thin films", // *J.Appl.Phys.*, 87(8), 3941-3949, (2000).
10. K. Aoki, Y. Fukuda, K. Numata, A. Nishima, A. Nishimura, "Dielectric properties of (111) and (100) lead zirconate titanate thin films prepared by sol-gel technique", // *Jpn.J.appl.Phys.part.1*, 33(9B), 5155-5158, (1994).
11. R. Kurchania, S.J. Milne, "Characterization of sol-gel Pb(Zr_{0.53}Ti_{0.47})O₃ films in thickness range 0.25-10µm", // *J.Mater.Res.*, 14(5), 1852-1859, (1999).
12. H-J. Nam, H-H.Kim, W-J.Lee, "The effects of the preparation conditions and the heat treatment conditions of Pt/Ti/SiO₂/Si substrates on the nucleation and growth of Pb(Zr,Ti)O₃ thin films", // *Jpn.J.appl.Phys.*, 37(6A), 3462-3470, (1998).
13. B. Jaber, D. Remiens, B. Thierry, "Substrate temperature target composition effects on PbTiO₃ produced in-situ by sputtering", // *J.Appl.Phys*, 79(4), 1182-1187, (1996).
14. G. Velu, D. Remiens, "Electrical properties of sputtered PZT films on stabilized platinum electrodes", // *J.Europ.Ceram.Soc.*, 19, 2005-2015, (1999).
15. G.Velu, D. Remiens, B. Thierry, "Ferroelectric properties of PZT film prepared by sputtered with stoichiometric single oxide target : comparison between conventional and RTA annealing", // *J.Europ.Ceram.Soc*, 1749-1758, (1997).
16. I. Stolichnov, A. Tagantsev, N. Setter, S.S. Okhonin, P. Fazan, J.S. Croos , M. Tsukada, "Dielectric breakdown in (Pb,L) (Zr,Ti)O₃ ferroelectric thin films with Pt and oxide electrodes", // *J.Appl.Phys*. 87(4), 1925-1931, (2000).
17. K.H. Park, C.Y. Kim, Y.W. Jeong, H.J.K. Won, K.Y. Kim, J.S. Lee, S.T. Kim, "Micro structures and interdiffusion of Ti/Pt electrodes with respects to annealing in the oxygen ambient", // *J.Mater.Res.*, 10(7), 1791-1794, (1995).
18. H-J.Nam, D-K.Choi, W-J.Lee, "Formation of hillocks on Ti/Pt electrodes and their effects on short phenomena of PZT films deposited by reactive sputtering", // *Thin Solid Films*, 371, 264-271, (2000).
19. J.C. Kim, D.S. Yoon, J.S. Lee, C.G. Choi, K. No, "A study on the micro structure of the preferred orientation of lead zirconate titanate (PZT) thin films", // *J.Mater.Res*. 12(4), 1043-1047, (1997).
20. K.G. Brooks, I.M. Reaney, R. Klissurka, Y. Huang, L. Bursill, N. Setter, "Orientation of rapid thermally annealed lead zirconate titanate thin films on (111) Pt substrates", // *J.Mater.Res.*, 9(10), 2540-2553, (1994).
21. D.V. Taylor, D. Damjanovic, "Piezoelectric properties of rhomboedral Pb(Zr,Ti)O₃ thin films with (100) and (111) and "random crystallographic orientation", // *Appl.Phys.Lett.*, 76(12), 1615-1617, (2000).
22. H.D.Chen, K.R.Udayakumar, C.J. Gaskey, L.E. Cross, J.J. Bernstein, L.C. Niles, "Fabrication and electrical properties of lead zirconate titanate thick films", // *J.Am.Ceram.Soc.*, 79(8), 2189-2192, (1996).
23. H. Fujisawa, S. Nakashima, M. Shimuzu, H. Niu, "Dependence of electrical properties of Pb(Zr,Ti)O₃ thin films on the grain size and film thickness", // *Proc. Of the 11th Int. Symp. on Applications of Ferroelectrics -ISAF-*, 77-80, (1998).
24. H.J. Kim, J.H. Oh, H.M. Jang, "Thermodynamic theory of stress distribution in epitaxial Pb(Zr,Ti)O₃ thin films", // *Appl.Phys.Lett.*, 75(20), 3195-3197, (1999).
25. D.Fu, T. Ogawa, H. Suzuki, K. Ishikawa, "Thickness dependence of stress in lead titanate thin films deposited on Pt-coated Si", // *Appl.Phys.Lett.*, 77(10), 15321534, (2000).
26. J.L. Deschanvre, P. Rey, G. Delabouglise, M. Labeau, "Characterization of piezoelectric properties of zinc oxide thin films deposited on silicon for sensors applications", // *Sensors & Actuators*, A33, 43-45, (1992).
27. A.L. Kholkin, C. Wutchrch, D.V. Taylor, N. Setter, "Interferometric measurements of electric field-induced displacement in piezoelectric thin films", // *Rev.Sci.Instrum.*, 65(5), 1935-1941, (1996).
28. H. Okino, T. Nishikawa, M. Shimuzu, T. Horiuchi, K. Matsushige, "Electrical properties of highly strained epitaxial Pb(Zr,Ti)O₃ thin films on MgO (100)", // *Jpn.J.Appl.Phys.*, 38(9B), 5388-5391, (1999).
29. C.R. Cho, W.J. Lee, B.G. Yu, B.W. Kim, "Dielectric and ferroelectric response as a function of annealing temperature and the film thickness of sol-gel deposited Pb(Zr_{0.52}Ti_{0.48})O₃ thin films", // *J.Appl.Phys.*, 86(5), 2700-2711, (1999).
30. S-I. Hirano, T. Yogo, K. Kikuta, Y. Araki, M. Saitoh, S. Ogasahara, "Synthesis of highly oriented lead zirconate-lead titanate films using metallo-organic", // *J.Am.Ceram.Soc.*, 75(10), 2785-2789, (1992).
31. F. Fujisawa, S. Nakashima, K. Kaibara, M. Shimuzu, H. Niu, "Size effects of epitaxial and polycrystalline Pb(Zr,Ti)O₃ thin films grown by metalorganic chemical vapor deposition", // *Jpn.J.appl.Phys.*, 38(9B), 53925396, (1999).
32. F. Xu, S. Trolrier-Mckinstry, W. Ren, B. Xu, Z-L. Xie, K.J. Hemker, "Domain wall motion and its contribution to the dielectric and piezoelectric properties of PZT films", // *J.Appl.Phys.*, 89(2), 1336-1349, (2000).
33. S. Hiboux, P. Muralt, "Piezoelectric and dielectric properties of sputter deposited (111), (100) and random oriented Pb(Zr_xTi_{1-x})O₃ (PZT) thin films", // *Ferroelectrics* 224(1-4), 315-322, (1999).
34. S.Y. Chen, I.W. Chen, "Comparative role of metalorganic decomposition -derived [100] and [111] in electrical properties of Pb(Zr,Ti)O₃ thin films", // *J.Am.Ceram.Soc.*, 36(7A), 4451-4458, (1997).
35. A.L. Kholkin, K.G. Brooks, D.V. Taylor, S. Hiboux, N. Setter, "Self-polarization effects in Pb(Zr,Ti)O₃ thin films", // *Int.Ferroelectrics*, 22(1-4), 525-533, (1998).
36. K.Lefki, G.J.M. Dormans, "Measurement of piezoelectric coefficients of ferroelectric thin films", // *J.Appl.Phys.*, 76(3), 1764-1767, (1994).
37. E. Cattan, T. Haccart, D. Remiens, "e₃₁ piezoelectric constant measurement of lead zirconate titanate thin films", // *J.Appl.Phys.*, 86(12), 7017-7023, (1999).

T. Haccart et al.: Dielectric, ferroelectric and piezoelectric properties...

38. A.L. Kholkin, A.K. Tagantsev, E.L. Colla, D.V. Taylor, N. Setter, "Piezoelectric and dielectric aging in $\text{Pb}(\text{Zr,Ti})\text{O}_3$ thin films and bulk ceramics", // *Int.Ferroelectrics*, 15, 317-324, (1997).
39. K. Carl, K.H. Hardtl, "Electrical after effects in $\text{Pb}(\text{Zr,Ti})\text{O}_3$ ceramics", // *Ferroelectrics* 17, 473-486, (1978).
40. S. Sun, Y. Wang, P.A. Frierer, B.A. Tuttle, "Annealing effects on the internal bias field in ferroelectric PZT thin films with self-polarization", // *Int.Ferroelectrics*, 23, 25-43, (1999).
41. U. Robels, L. Schneider-Stormann, G. Arlt, "Domain wall trapping as a result of internal bias fields", // *Ferroelectrics* 133,(1-4), 223-228, (1992).
42. W.L. Warren, B.A. Tuttle, D. Dimos, G.E. Pike, H.N. Al-Shareef, R. Ramesh, J.J.T. Evans, "Imprint in ferroelectric capacitors", // *Jpn.J.appl.Phys.*, 35(Part.1-2B), 1521-1524, (1996).
43. M.V. Raymond, D.M. Smyth, "Defects and charge transport in perovskite ferroelectrics", // *J.Phys.Chem.Solids*, 57(10), 1507-1511, (1996).
44. B. Jaber, E. Cattan, P. Tronc, D. Remiens, B. Thierry, "Piezoelectric properties of sputtered PbTiO_3 films : growth temperature and poling treatment effect", // *J.Vac.Sci.Tech.*, A16(1), 144-152, (1998).
45. C. Lee, T. Itoh, T. Suga, "Characterization of micro mechanical piezoelectric PZT force sensors for dynamic scanning force microscopy", // *Rev.Sci.Instrum.* 68(5), 2091-2100, (1997).